



Rilevamento di precursori di esplosivi con tecnologia Lidar ad assorbimento differenziale mediante oscillatore parametrico ottico

Il presente studio è mirato allo sviluppo di un sensore laser remoto capace di rilevare i precursori utilizzati per fabbricare dispositivi esplosivi improvvisati (IEDs). Dopo uno studio spettroscopico preliminare in una cella di assorbimento, la fattibilità di un Lidar/DIAL (Differential Absorption Lidar) per il rilevamento di vapori di acetone è stata studiata in laboratorio, simulando le condizioni di campagne sperimentali sul campo. Infine, tenendo conto di misurazioni effettuate in uno scenario reale, è stato eseguito uno studio su eventuali interferenti atmosferici, ricercando tutti i composti noti che hanno in comune l'assorbimento nell'infrarosso (IR) dell'acetone nella banda spettrale selezionata per poterne rilevare la presenza. Possibili specie interferenti sono state studiate simulando sia un ambito urbano sia uno industriale: valori limite di rilevamento di acetone sono stati individuati in entrambi i casi. Lo studio qui descritto ha confermato che un Lidar/DIAL è in grado di rilevare acetone a bassa concentrazione anche a distanze notevoli.

Differential Absorption Lidar detection of explosive precursors by Optical Parametric Oscillator laser systems

The present study is aimed at the development of a laser remote sensor able to detect precursors employed in the manufacturing of IEDs (Improvised Explosive Devices). After a preliminary spectroscopic study in an absorption cell, the feasibility of a lidar/DIAL (Differential Absorption Lidar) for the detection of acetone vapors has been investigated in laboratory, simulating the experimental conditions of a field campaign. Eventually, having in mind measurements in a real scenario, a study of possible atmospheric interferents has been performed, looking for all known compounds that share with acetone infrared (IR) absorption in the spectral band selected for its detection. Possible interfering species were investigated simulating both urban and industrial atmospheres, and limits of acetone detection in both environments were identified. This study confirmed that a lidar/DIAL can detect low-concentration acetone at considerable distances.

DOI: 10.12910/EAI2014-89

■ A. Puiu, L. Fiorani, R. Borelli, M. Pistilli, O. Rosa, A. Palucci

Introduction

Terrorist bombings in the last few years led to an increased demand for the development of new technologies able to prevent such events. In particular,

■ Contact person: Luca Fiorani
luca.fiorani@enea.it



FIGURE 1 On 22nd July, 2011, the government buildings in Oslo were bombed (left picture) [livinginphilistia.blogspot.it], resulting in eight casualties. The bomb was made in a farmhouse (top right picture) [lionheartuk.blogspot.it] from fertilizer (bottom-right picture) [news.images.itv.com] and other explosive precursors

a remote sensor could have detected explosive precursors escaping from the farmhouse where the Oslo bombing was prepared (Fig. 1). Prevention means rapid identification of illegal bomb factories employed to produce IEDs, often based on triacetone triperoxide (TATP). Nowadays, this is possible thanks to the emerging remote sensing technologies based on recently developed laser sources.

In this work we report on acetone detection by means of a lidar/DIAL based on an Optical Parametric Oscillator (OPO) laser system, in the framework of the project BONAS (BOmb factory detection by Networks of Advanced Sensors). We used the “IR Opolette HE 3034” model by Opotek, that has the benefit of being a portable compact laser source tunable in the range 3 – 3.45 μm , where both TATP and its precursor acetone have quite strong absorption peaks. TATP ($\text{C}_9\text{H}_{18}\text{O}_6$) is a powerful explosive, easy to make using commonly available chemicals, such as acetone ($\text{C}_3\text{H}_6\text{O}$) and hydrogen peroxide (H_2O_2). Being not difficult to synthesize, TATP is often the explosive of choice for terrorists [1].

TATP is one of the most dangerous explosives known, being extremely sensitive to impact, temperature

change and friction. Just a few hundred grams of the material produce hundreds of liters of gas in a fraction of a second [2]. Thus, the development of sensing systems able to identify illegal factories where IED are produced turns out to be of critical importance for the security of people and territory. The present research is focused on the remote detection of acetone, which can be identified in its vapor state outside the building where TATP is prepared.

Spectroscopy of acetone

Acetone (molecular weight: 58.0791 g mol^{-1}) is a colorless liquid, flammable and irritant with a high vapor pressure (24,600 Pa at 20 $^\circ\text{C}$) [3]. Absorption spectra of acetone and TATP measured by Diffuse Reflectance Infrared Fourier Transform (DRIFT) spectroscopy [4] put in evidence that both substances exhibit many absorption peaks in the spectral interval from 3 to 10 μm .

Acetone has a few stronger absorption bands around 5.8 μm (C=O stretch), 7.3 μm , 8.2 μm (skeletal vibrations) and 18.85 μm , as well as weaker absorption bands at 3.4 μm (C–H stretch), 6.97 μm , 9.1 μm and 11.2 μm .

This is not surprising because generally, in an infrared (IR) spectrum, the less polar C–H bond has smaller absorption intensity than the more polar C=O bond. The region from 6.5 to 20 μm – called the ‘fingerprint region’ – usually contains a very complicated series of absorptions which are mainly due to all manner of bending vibrations within the molecule. It is much more difficult to pick out individual bonds in this region than it is in the clearer region at lower wavelengths (under 6.5 μm). In lidar atmospheric sensing, it is important to take into account not only the spectroscopic features of the species to be revealed, but also the spectroscopy of the atmosphere. For this reason, we performed transmittance simulations of acetone vapor, based on “The NIST Chemistry WebBook” [3, 5] and atmosphere, based on the “U.S. Standard Atmosphere, 1976” [6]. This study showed that the most intense absorption bands of acetone, free of atmosphere interference, are centered at 3.4 μm and 8.2 μm .

The spectral range below 2.5 μm was not considered in this simulation because it is characterized only by weak overtone bands of acetone. The 2.5 – 3 μm and 5 – 7.5 μm spectral windows are dominated by water, while the 4.1 – 4.5 μm band is completely covered by a strong carbon dioxide absorption and has no acetone

spectral features. The ‘fingerprint region’ is considered an important spectral window because each different compound produces a different pattern of troughs in this particular region of the IR spectrum. The only problem to reveal acetone in the fingerprint region is its possible interference with other components of the atmosphere. In fact, at wavelengths longer than 14 μm , gases such as CO_2 and CH_4 (along with less abundant hydrocarbons) absorb strongly due to the presence of relatively long C–H and carbonyl bonds, as well as water vapor, that absorbs in rotation modes. As a consequence, acetone could potentially be detected using a lidar/DIAL system at wavelengths near 3.4 μm , 8.2 μm , 9.15 μm and 11.15 μm . Yet, in a real scenario we must consider that the presence of the IR radiation background may have a negative effect on the signal-to-noise ratio (SNR) of the instrument. The main contributions to IR background come from down-going solar radiation (IR energy coming from the Sun) and from up-going thermal radiation (IR energy coming from the Earth). By computing radiative transfer in the Earth’s atmosphere with SBDART WebTool [7] it can be noticed the IR background is higher at longer wavelength. Taking into account the above spectroscopic considerations (related to atmosphere, acetone, IR background) and the requirement for a compact tunable unit with high pulse energy ($> 3 \text{ mJ}$) and good beam quality (linewidth $< 10 \text{ cm}^{-1}$), OPO turns out to be the proper light source for lidar detection of acetone. The OPO manufactured by Opotek has been chosen because of its ease of use, operational reliability, small volume and low weight. Nowadays, due to the development of the quantum cascade laser (QCL) technology [8], compact tunable laser sources working at room temperature are available from 2.75 μm to 16 μm , but the emitted energy is still too low for long-range remote sensing.

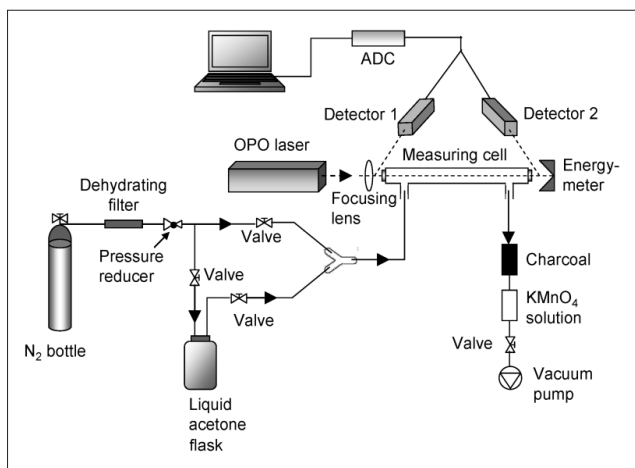


FIGURE 2 Table top set-up for spectroscopic measurements. ADC: analog-to-digital converter. The detectors are very sensitive and were illuminated by the small amount of radiation scattered by focusing lens (detector 1) and energy meter (detector 2), and no beam-splitter was used

Experimental set-up for in-cell acetone detection

In order to measure the transmission spectrum of vapor phase acetone at OPO emission wavelength, a table top experimental set-up was realized in our laboratory (Fig. 2). A glass cell (1.5 m long) closed by two ZnSe

windows was filled with different concentrations of acetone. The vapors, produced in the flask containing pure liquid acetone (99.98% by Carlo Erba) at room temperature, were transported by a nitrogen flux into the measuring cell. The laser beam was slightly

focused into the cell by a ZnSe lens and dumped on the energy-meter. The transmittance of the cell was measured by two detectors placed before and after the cell. At the cell exit, charcoal and/or KMnO_4 solution were introduced for safety reasons, to reduce the vapor

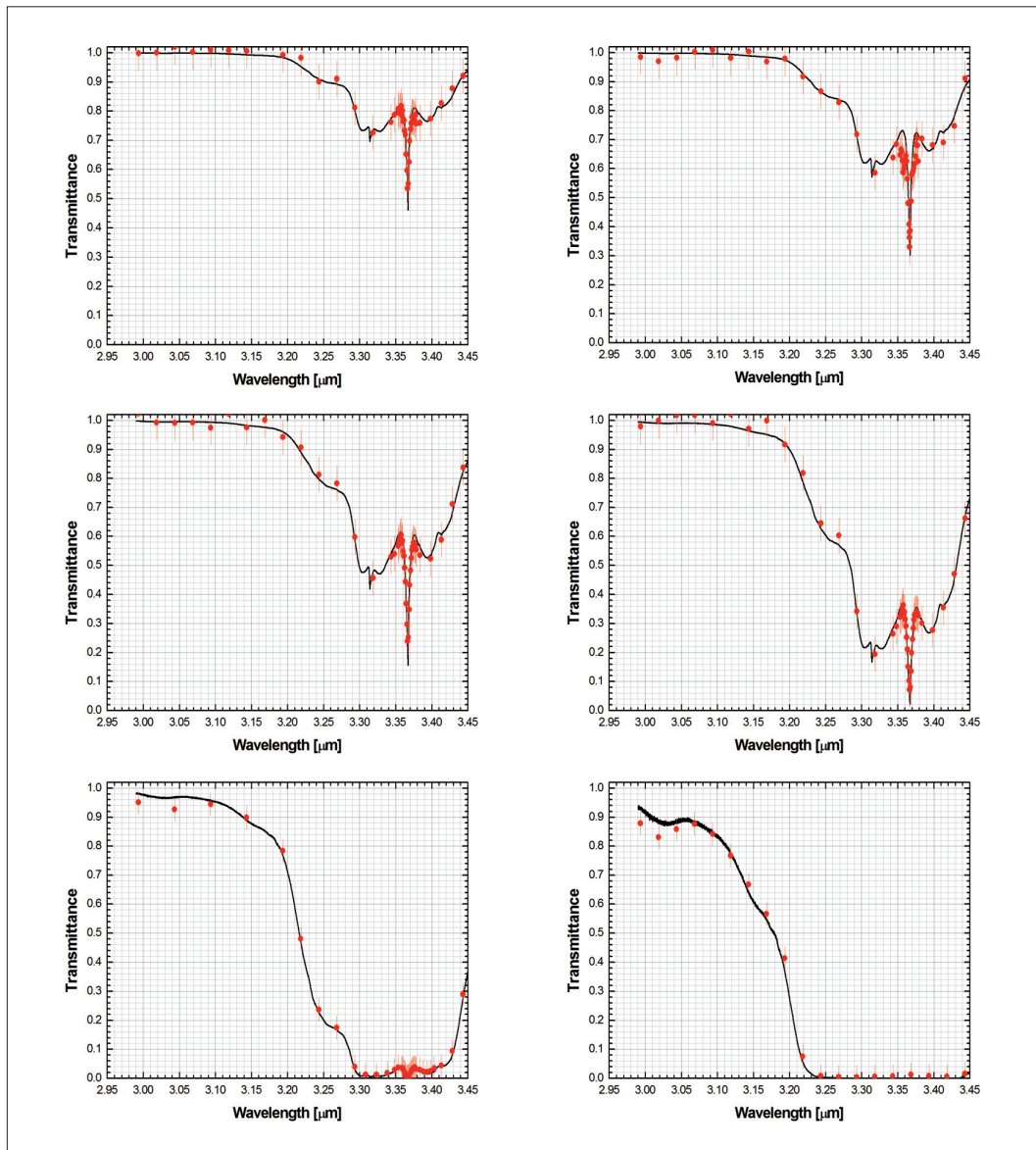


FIGURE 3 Transmittance of acetone measured at ENEA (dots) and according to the PNNL database (line) for six different concentrations: 1700 ppm (top left), 2600 ppm (top right), 3800 ppm (middle left), 8000 ppm (middle right), 25,000 ppm (bottom left) and 100,000 ppm (bottom right)

emissions of the explosive precursor under study. The transmittance at a given wavelength has been obtained averaging 100 laser shots. Only a small part of the laser energy was used for the cell measurements (the OPO is equipped with a variable attenuator). The measured spectra were compared in Figure 3 with the Pacific Northwest National Laboratory (PNNL) database [10], that is more recent and has finer resolution with respect to the database [5] available in “The NIST Chemistry WebBook” [3].

The agreement between experimental measurement and PNNL data is good, especially for low transmittance. This is not surprising: high transmittance corresponds to small differences between the signal before and after the cell, more sensitive to the noise. The OPO by Oportek proved to be not only light-weight and compact, but also user-friendly and reliable. This makes the integration of this OPO laser into a portable lidar system possible. All these results confirm that OPO sources are good candidates for lidar/DIAL detection of IED precursors in real scenarios.

Lidar/DIAL measurements

A typical lidar system uses a laser to propagate a light pulse to a transparent or hard target. A fraction of the back-scattered light is collected by a telescope and focused onto a detector. The signal from the detector is then analyzed with the aid of high speed electronics to give information about the investigated atmosphere. A schematic of our lidar configuration is shown in Figure 4. Pump laser and OPO are integrated into a single compact unit, which is cooled by closed cycle water. The laser is a flash lamp pumped Nd:YAG emitting 1064 nm radiation with a pulse repetition rate of 20 Hz, a pulse length of 7 ns and a beam diameter of 4 mm. The OPO system has a maximum pulse energy of 3.4 mJ. The OPO beam characteristics – full angle

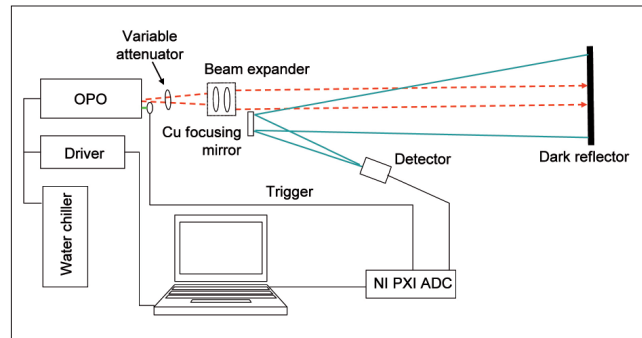


FIGURE 4 Schematic set-up of the laboratory OPO-lidar system. NI: National Instruments, PXI: PCI (Peripheral Component Interconnect) extensions for instrumentation. The trigger signal is provided by a photodiode observing the Nd:YAG pulse

divergence, waist beam size and beam quality factor – as measured in our lab, are reported in Table 1.

In order to avoid detector saturation, we placed a variable attenuator on the beam path. The beam expander was used in order to match the transmitter divergence with the receiver field of view, as well as for eye safety reasons. In fact, according to the Directive 2006/25/EC of the European Parliament, for the following conditions:

- a) laser exposure to the eye less than 10 s,
- b) laser pulse duration from 1 to 100 ns,
- c) wavelength range from 2.6 to 1000 μm ,

the maximum permissible exposure MPE is 100 J/m². Having in mind that a typical laser footprint is about 1 cm², the maximum energy dose is around 10 mJ. If more than three shots of our system at its maximum energy are fired in one direction, the laser footprint has to be enlarged accordingly, and this can be easily accomplished by using a beam expander: at its output the diameter of the laser spot is about 1.2 cm, corresponding to 1 cm².

The lidar specifications are summarized in Table 2.

Laser parameter	Full angle divergence θ (mrad)	Waist beam size D_0 (mm)	Beam quality factor M^2
Horizontal	8.7	0.47	1.004
Vertical	6.0	0.68	1.005

TABLE 1 Laser beam features

Subsystem	Characteristics	
Transmitter ("IR Opolette HE 3034" model by Opotek)	Wavelength	3362 nm
	Attenuated pulse energy	0.15 mJ
	Pulse duration	10 ns
	Pulse repetition rate	20 Hz
Cu focusing mirror (manufactured in our lab)	Diameter	8 mm
	Focal length	197.5 mm
Detector ("PVI-4TE-3.4" model by Vigo)	Size	1×1 mm ²
	Detectivity	9.2×10 ¹¹ cm Hz ^{1/2} /W
ADC ("PXIe-5122" model by NI)	Sampling frequency	100 MS/s
	Vertical resolution	14 bit

TABLE 2 Specifications of OPO-lidar system

Laboratory tests for lidar/DIAL detection of acetone vapors

The laboratory tests were performed in order to assess the acetone concentration that could be found close to a window or an aeration duct of an illegal IED factory. For this, liquid acetone was placed in an uncovered glass Petri dish (diameter: 0.2 m) just below the laser beam, so the released vapor intercepted the laser beam.

The measurements were carried out in the following laboratory conditions: temperature T = 294.45 K; pressure P = 98,200 Pa; optical path ΔR = 0.2 or 6.35 m. The values 0.2 and 6.35 m correspond to the measurements carried out just after pouring acetone into the dish and waiting it to diffuse in the whole room, respectively. In fact:

- just after pouring acetone, we can assume that its vapors are present just over the Petri dish, i.e. in an optical path of 0.2 m;

Test data	Range ΔR [cm]	Measurement-derived acetone concentration [molecule/cm ³]	Measurement-derived acetone concentration [ppm]
[data1]	20	5.8×10 ¹⁸	240,660
[data2]	635	4.3×10 ¹⁷	17,842
[data3]	635	5.4×10 ¹⁷	22,407
[data4]	635	6.9×10 ¹⁷	28,630

TABLE 3 Results of laboratory test for lidar/DIAL detection of acetone vapor

- once acetone is diffused in the room, its vapors are distributed in all the optical path between transmitter and reflector (their distance is 6.35 m).

By applying to the Lambert-Beer law the records for acetone given by the PNNL database (acetone concentration N_{ac} = 10⁻⁶ atm; optical path L = 100 cm, acetone absorbance at 3362 nm A = 8.59×10⁻⁷), and knowing the number of molecules of the standard atmosphere N_{atm} = 2.46×10¹⁹ molecule/cm³, the acetone cross section (σ) at 3362 nm was calculated to be 3.49×10⁻²² cm²/molecule.

The first measurement (data1) was performed out just after pouring acetone while data2 – data4 were temporally spaced by a few minutes interval between them. The calculated acetone concentrations for the sequence of four acquisitions are reported in Table 3.

Knowing that the acetone diffusion coefficient in the air is 0.124 cm²/s, we can assume that a short time after [data2], [data3] and [data4] were acquired, acetone diffusion covered all the range ΔR = 635 cm. As one can expect, the concentration of data1 is close to the acetone vapor pressure (246,000 ppm), while the average concentration in the room grows over time (data2 to data4).

Considering the case of a vapor plume near a bomb factory, it is reasonable to assume that the concentration is between 1 and 10%, i.e. we expect to find values of acetone concentration on the field between 2460 and 24,600 ppm. As can be noticed, the laboratory tests confirm that our OPO lidar system is a good candidate

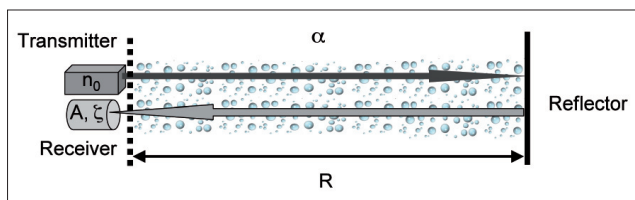


FIGURE 5 Lidar principle of operation in the presence of a hard target

for detecting such quantities of acetone. From the lidar equation [9] we can conclude that using a 300-mm telescope and removing the OPO attenuator (3 mJ instead of 0.15 mJ) 200 ppm of acetone should be detected at 1.5 km.

Received power and signal to noise ratio

In general, the backscattered lidar returns from a hard target are about six orders of magnitude higher than that from aerosols in the atmosphere. In the following, we shall consider the case of a hard target experiment (Fig. 5).

As a reflector (target) we used a rough dark surface of SBR (Styrene-Butadiene Rubber) composite. Usually, not all rough surfaces are Lambertian reflectors, but this is often a good approximation when the characteristics of the surface are unknown. If we consider a Lambertian surface where the target area is greater than or equal to the beamwidth and the receiver field of view is greater than or equal to the transmitter beamwidth [11], the lidar signal or power received or backscattered from a hard target (P_r) may be described by the Lidar Equation [9], [26], [27]. All the parameters used to calculate the received power for acetone detection with the experimental set-up described in Figure 4 were reported elsewhere [26], [27]. With this parameters, the calculated number of the received photons n_r was 8.2×10^{14} . Knowing that the energy of a single photon is $E = hc/\lambda$, for n_r photons we obtain a received power P_r of 5×10^{-5} W. The measured received power is given by the ratio between the acetone signal S [V] and the product of detector transimpedance T [V/A] and current responsivity R_i [A/W] at the laser wavelength of 3362 nm. Taking into account that the recorded acetone signal was 1.12 V,

the measured received power results to be 6×10^{-5} W, very close to the calculated value (5×10^{-5} W). The equation and parameters used for the calculation of SNR were previously reported [26], [27]. A very good SNR was obtained (1.68×10^6).

Study of possible atmospheric interfering molecules in real scenarios

In this section we shall analyze the molecules normally present in the atmosphere which may interfere with acetone detection. For this study, we have chosen as a reference the US standard atmosphere [6] due to the richness of available data furnished by different Institutions, such as EPA (US Environmental Protection Agency) [13] and CDIAC (Carbon Dioxide Information Analysis Center) [14]. For the research of reference spectra of the selected interfering molecules, HITRAN [12] and NIST (National Institute of Standards and Technology) [3] databases were used. The molecules which may interfere with acetone detection (see Table 4) were selected taking into account their absorption coefficients for each compound (at standard atmospheric concentrations).

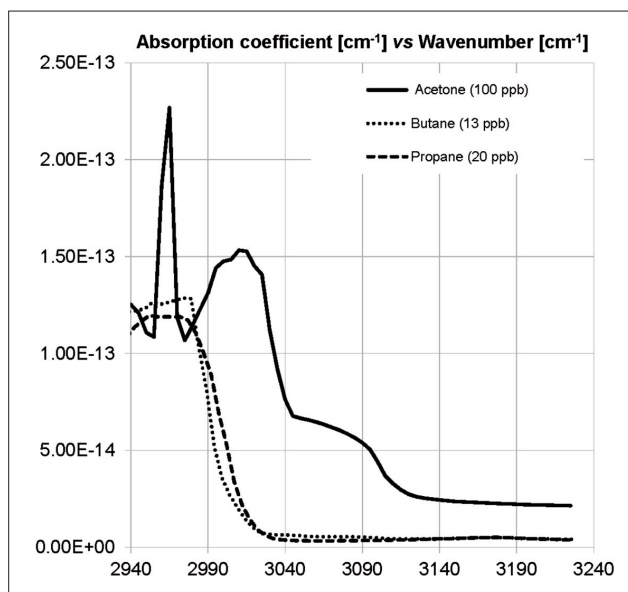


FIGURE 6 Simulation of molecular species interfering with 100 ppb of acetone in urban areas

Classes	Name	Formula	Database	Concentration (ppb)	Reference
Alkanes	Butane	C ₄ H ₁₀	Nist	13.00	[15]
	Propane	C ₃ H ₈	Nist	20.00	[15]
	Pentane	C ₅ H ₁₂	Nist	0.207	[16]
Alkenes	1,3butadiene	C ₄ H ₆	Nist	0.4	[17]
	Propene	C ₃ H ₆	Nist	1.33	[18]
	Acetylene	C ₂ H ₂	Nist	1.622	[18]
Alcohol	Isopropyl Alcohol	C ₃ H ₈ O	Nist	0.604	[18]
Epoxide	Ethylene Oxide	C ₂ H ₄ O	Nist	0.005	[19]
Aldehydes	Formaldehyde	C ₂ HO	Hitran	2.33	[20]
	Benzene	C ₆ H ₆	Nist	0.22	[18]
Aromatic Hydrocarbons	Toluene	C ₇ H ₈	Nist	0.42	[18]
	Strene	C ₈ H ₈	Nist	0.1889	[21]
	Ethylbenzene	C ₈ H ₁₀	Nist	0.05	[18]
Chloro Compounds	Chloromethane	CH ₃ Cl	Nist	0.7	[17]
	Dichloromethane	CH ₂ Cl ₂	Nist	0.2	[17]
	Ethylene Dichloride	C ₂ H ₄ Cl ₂	Nist	0.1	[17]
	Methyl Chloroform	C ₂ H ₃ Cl ₃	Nist	0.113	[17]
	Chloroethene	C ₂ H ₅ Cl	Nist	3.3x10 ⁻³	[22]
	Tetrachloro-ethylene	C ₂ Cl ₄	Nist	0.1	[17]
	Tetrachloro-methane	CCl ₄	Nist	0.13	[23]
	Chloroform	CHCl ₃	Nist	0.1	[17]
Halons Compounds	Ethylene Dibromide	C ₂ H ₄ Br ₂	Nist	0.02	[19]
	Methyl Iodine	CH ₃ I	Nist	0.002	[24]
Sulfur Compounds	Carbonyl Sulfite	OCS	Nist	0.466	[25]
	Carbon Disulfide	CS ₂	Nist	0.038	[26]
Nitrogen Compounds	Nitrogen Dioxide	NO ₂	Nist	11.44	[24]
	Ethyl Nitrate	C ₂ H ₅ NO ₃	Nist	0.003	[20]

TABLE 4 List of selected interfering molecules

In Table 4 the compounds mostly cited in literature as present in the atmosphere at measurable levels are listed. From this study we excluded the pollutants having no spectral features in the wavelengths range covered by OPO, such as: sulfur dioxide (SF₆), bromotrifluoromethane (CBrF₃), chlorodifluoromethane (CHClF₂), dichlorofluoromethane (CCl₂F₂), fluoroform (CHF₃), bromoclorodifluoromethane (CF₂ClBr), 1-chloro 1,1-difluoroethane (C₂H₃F₂Cl), methyl bromide

(CH₃Br), dichlorodifluoroethane (C₂H₂Cl₂F₂), and sulfur dioxide (SO₂).

Having in mind the considerations made so far, we shall examine the feasibility of a lidar/DIAL detection of acetone in different environments. Two scenarios (urban and industrial atmospheres) have been considered.

By simulating acetone in urban atmosphere (Fig. 6), we obtained that for acetone concentrations ≤100

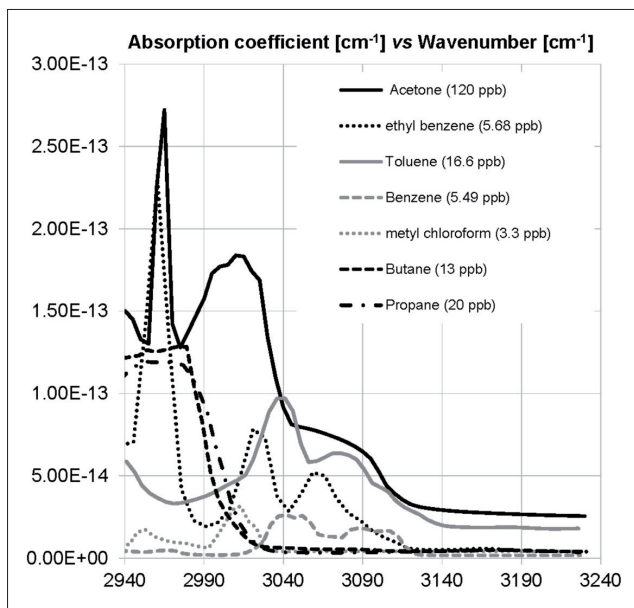


FIGURE 7 Simulation of molecular species interfering with 120 ppb of acetone in industrial areas

ppb, butane and propane absorption profiles start to interfere with acetone measurement.

If we suppose a scenario in which we have to measure acetone in a very polluted atmosphere, such as an industrial area, we found that ethyl-benzene and toluene start to interfere for acetone concentrations ≤ 120 ppb (Fig. 7), while butane and propane absorption remains unchanged.

In summary, in industrial areas, when dealing with an acetone concentration of about 120 ppb, we may find four main interfering species: butane, propane, ethyl-benzene and toluene; but this is not limitative since not all the spectral interval where OPO emits is covered by interfering species. In principle, by choosing two appropriate wavelengths ($\lambda_{ON} \sim 3010 \text{ cm}^{-1}$ and $\lambda_{OFF} \sim 3145 \text{ cm}^{-1}$), a lidar/DIAL system can be employed to detect acetone in concentrations of the order of 100 ppb.

Conclusions

The aim of this work was to prove the capability of the developed lidar/DIAL system to measure precursors of IEDs, such as acetone nearby illegal factories. From the spectroscopic considerations on acetone, we may conclude that the best spectral bands for acetone detection are centered around 3.4 and 8 μm . The spectral interval from 3.1 to 3.45 μm , investigated with a laser having $\Delta\lambda \sim 10 \text{ cm}^{-1}$, was chosen, as this spectral region is almost free from atmospheric interference and solar background. Laboratory tests were performed in order to monitor acetone with an OPO lidar/DIAL system. Results indicate that the measured signal coincide with the ones derived from the performed measurements by about 10%, and the detection limit is 200 ppm of acetone at a range of 1.5 km.

From the study of possible atmospheric interfering molecules in a real scenario, we can conclude that it is possible to measure acetone in both scenarios: urban and industrial environments till 120 ppb with no risk of false positive. Moreover, by using a compact laser source, the laboratory set-up can be easily integrated into a portable system for on-field measurements.

Acknowledgements

The support from the EU-FP7 BONAS project (contract no. 261685) is gratefully acknowledged.

Within the BONAS project a joint experimental test has been arranged at the AM-CSV (Italian Military Aeronautics - Experimental Flight Center) facility at Pratica di Mare airport, the logistic support and participation from AM personnel is kindly acknowledged.

Adriana Puiu, Luca Fiorani, Rodolfo Borelli, Marco Pistilli, Olga Rosa*, Antonio Palucci

ENEA, Technical Unit for the Development of Applications of Radiation - Diagnostics and Laser Metrology Laboratory
* guest student



- [1] I. Dunayevskiy, A. Tsekoun, M. Prasanna, R. Go, C.K.N. Patel, 2007, *Appl. Opt.*, 46, 6397.
- [2] <http://www.globalsecurity.org/military/systems/munitions/tatp.htm>
- [3] P.J. Linstrom, W.G. Mallard, 2001, *J. Chem. Eng. Data*, 46, 1059.
- [4] A. Puiu, G. Giubileo, S. Nunziante Cesaro, 2012, *Int. J. Spec.*, 953019.
- [5] A.L. Smith, 1982, *The Coblenz Society Desk Book of Infrared Spectra*, Second Edition, The Coblenz Society Kirkwood US.
- [6] U.S. Standard Atmosphere, 1976, United States Government Printing Office Washington, US.
- [7] P. Ricchiazzi, S. Yang, C. Gautier, D. Sowle, 1998, *Bull. Am. Met. Soc.*, 79, 2101.
- [8] J. Faist, F. Capasso, D.L. Sivco, C. Sirtori, A.L. Hutchinson, A.Y. Cho, 1994, *Science*, 264, 553.
- [9] L. Fiorani, "Lidar application to lithosphere, hydrosphere and atmosphere", 2010, in *Progress in Laser and Electro-Optics Research*, V.V. Koslovskiy, ed. 21-75 Nova, New York US.
- [10] S.W. Sharpe, T.J. Johnson, R.L. Sams, P.M. Chu, G.C. Rhoderick, P.A. Johnson, 2004, *Appl. Spectrosc.*, 58, 1452.
- [11] G. Mamon, D.G. Youmans, Z.G. Sztankay, C.E. Mongan, 1978, *Appl. Opt.*, 17, 205.
- [12] L.S. Rothman, I.E. Gordon, A. Barbe, D.C. Benner, P.F. Bernath, M. Birk, V. Boudon, L.R. Brown, A. Campargue, J.P. Champion, K. Chance, L.H. Coudert, V. Dana, V. M. Devi, S. Fally, J.M. Flaud, R.R. Gamache, A. Goldman, D. Jacquemart, I. Kleiner, N. Lacome, W.J. Lafferty, J.Y. Mandin, S.T. Massie, S.N. Mikhailenko, C.E. Miller, N. Moazzen-Ahmadi, O.V. Naumenko, A.V. Nikitin, J. Orphal, V.I. Perevalov, A. Perrin, A. Predoi-Cross, C.P. Rinsland, M. Rotger, M. Šimecková, M.A.H. Smith, K. Sung, S.A. Tashkun, J. Tennyson, R.A. Toth, A.C. Vandaele, J. Vander Auwera, 2009, *J. Quant. Spectrosc. Radiat. Transfer*, 110, 533.
- [13] <http://www.epa.gov/ttnemc01/ftir/welcome.html>
- [14] http://cdiac.ornl.gov/oceans/LDEO_Underway_Database/
- [15] D.R. Worton, W.T. Sturges, C.E. Reeves, M.J. Newland, S.A. Penkett, E. Atlas, V. Stroud, K. Johnson, N. Schmidbauer, S. Solberg, J. Schwander, J.M. Barnola, 2012, *Atmospheric Environment*, 54, 592.
- [16] Department of Environment and Natural Resources, Ambient Monitoring Section, 2009 Ambient Air Quality Report, State of North Carolina, Report # 2012.01, May 2012.
- [17] Atmospheric Science Section of the Department of Environment and Conservation (NSW) of Australia, Ambient Air Quality Research Project 1996-2001, Internal working paper no. 2 "Ambient concentrations of toxic organic compounds in NSW".
- [18] B. Zielinska, W. Goliff, 2003, Final Report Central California Ozone Study - Volatile Organic Compounds Collection and Analysis by the Canister and Tenax Methods, Division of Atmospheric Sciences Desert Research Institute.
- [19] J.H. Seinfeld, S.N. Pandis, "Summary of the Average December 1977 Concentrations of Measured Trace Constituents Containing Halogens", in *Atmospheric Chemistry and Physics: From Air Pollution to Climate Change*, 1st Edition.
- [20] O. Hawas, D. Hawker, D. Cohen, E. Christensen, G. Golding, P. Vowles, 2002, *J. Chromatogr. A.*, 971, 173.
- [21] J.H. Seinfeld, S.N. Pandis, 2006, Status of Toxic Air Contaminant Identification (California Air Resources Board, *Atmospheric Chemistry and Physics: From Air Pollution to Climate Change*, 2nd Edition).
- [22] J.C. Low, N.Y. Wang, J. Williams, R.J. Cicerone, 2003, *J. of Geophysical Research*, 108, 4608.
- [23] Initial Statement of Reasons for Proposed Rulemaking State of California (California Environment Protection Agency, Air Resources Board Staff Report, February 2009).
- [24] N. Bell, L. Hsu, D.J. Jacob, M.G. Schultz, D.R. Blake, J.H. Butler, D.B. King, J.M. Lobert, and E. Maier-Reimer, 2002, *J. Geophys. Res.*, Vol. 107, No. D17, DOI: 10.1029/2001JD001151
- [25] P.J. Maroullis, A.L. Torres, A.R. Bandy, 1977, *Geophys. Research Letters*, 4, 510.
- [26] P.J. Maroullis, A.L. Torres, A.R. Bandy, 1980, *Geophys. Research Letters*, 7, 681.
- [27] L. Fiorani, A. Puiu, O. Rosa, A. Palucci, 2013, "Lidar/DIAL detection of bomb factories", in *Proc. of SPIE*, 8897, 889707-1.